





Modeling of Stress Concentration Factors in CFRP-Reinforced Circular Hollow Section KT-Joints Under Axial Compression [†]

Mohsin Iqbal ^{1,*}, Saravanan Karuppanan ¹, Veeradasan Perumal ¹, Mark Ovinis ², Muhammad Iqbal ³
and Adnan Rasul ¹

¹ Mechanical Engineering Department, Universiti Teknologi PETRONAS, Seri Iskandar 32610, Malaysia; saravanan_karuppanan@utp.edu.my (S.K.); veeradasan.perumal@utp.edu.my (V.P.); adnan_22006634@utp.edu.my (A.R.)

² College of Engineering, Birmingham City University, Birmingham B4 7XG, UK; mark.ovinis@bcu.ac.uk

³ College Department of Mechanical Engineering, CECOS University of IT & Emerging Sciences, Hayatabad, Peshawar 25000, Pakistan; muhammadiqbal@cecos.edu.pk

* Correspondence: mohsin_22005143@utp.edu.my; Tel.: +60-11-6509-8596

[†] Presented at the 5th International Electronic Conference on Applied Sciences, 4–6 December 2024; Available online: <https://asec2024.sciforum.net/>.

Abstract: Tubular structures are critical in renewable energy and offshore industries but face significant loads over time, leading to joint degradation. Carbon fiber-reinforced polymers (CFRPs) offer promising rehabilitation solutions, yet existing studies often overlook stress concentration factors (SCFs) along the weld toe. This study examines SCFs at 24 weld toe positions in CFRP-reinforced KT-joints under axial compression. Using 5429 simulations and artificial neural networks, precise estimations of CFRPs' impact on SCFs were achieved, with <10% error. These findings demonstrate CFRPs' potential to reduce SCFs and improve fatigue life prediction for tubular joints under axial compression.

Keywords: stress concentration factors (SCFs); carbon fiber-reinforced polymers (CFRPs); KT-joints; axial loads; hot-spot stress (HSS)



Academic Editor: Nunzio Cennamo

Published: 17 March 2025

Citation: Iqbal, M.; Karuppanan, S.; Perumal, V.; Ovinis, M.; Iqbal, M.; Rasul, A. Modeling of Stress Concentration Factors in CFRP-Reinforced Circular Hollow Section KT-Joints Under Axial Compression. *Eng. Proc.* **2025**, *87*, 19. <https://doi.org/10.3390/engproc2025087019>

Copyright: © 2025 by the authors. Licensee MDPI, Basel, Switzerland. This article is an open access article distributed under the terms and conditions of the Creative Commons Attribution (CC BY) license (<https://creativecommons.org/licenses/by/4.0/>).

1. Introduction

Circular hollow section (CHS) profiled structures are widely used in civil and offshore applications. These structures offer high specific strength, stiffness, and direction-independent structural responses [1]. Given their typically long service life and the dynamic nature of the loads that they are subjected to, fatigue strength is the primary design parameter. Over time, the repair or rehabilitation of these structures is required, especially for critical sections such as tubular joints, which are the connection points between two or more CHS members [2]. Similarly, design requirements are sometimes revised, necessitating the reinforcement of critical structural segments to meet updated load requirements. Reinforcement is also essential to extend the design life of structures that continue to operate beyond their service life. For example, numerous oil and gas rigs are used well beyond their design life to maximize profits [3].

While nominal member stresses may remain within allowable limits, the geometric variation at the tubular joint causes unequal deformation, and the presence of a weld notch leads to considerable stress amplification [4]. This behavior is illustrated in Figure 1. This phenomenon makes CHS joints the most critical component of tubular structures.

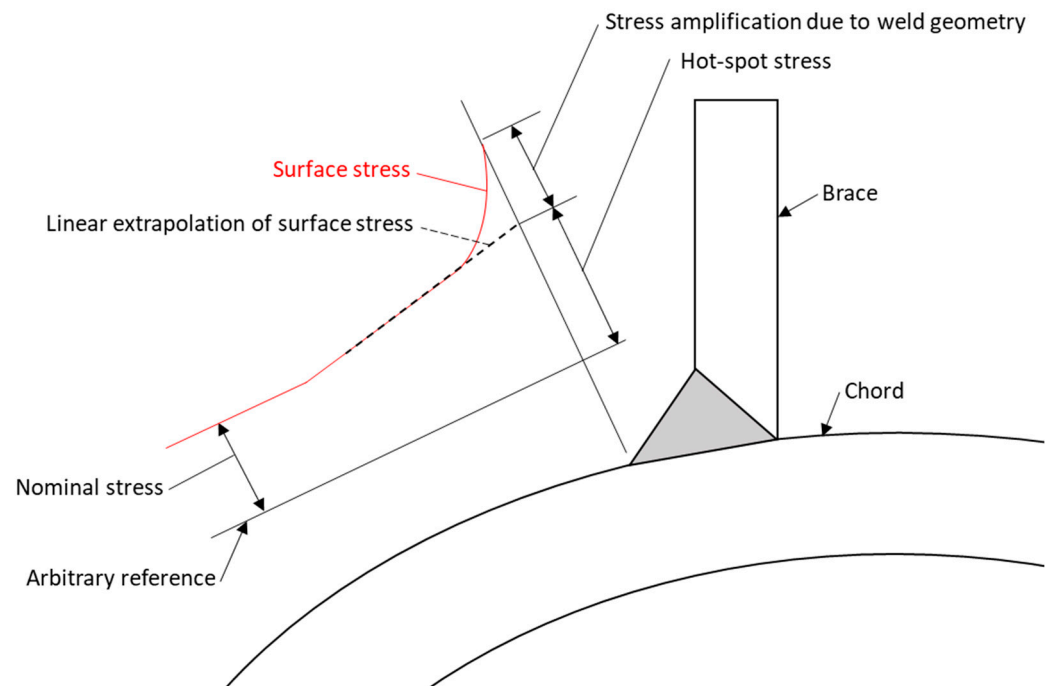


Figure 1. Stress behavior at a CHS joint.

When a joint in a structure deteriorates or faces load demands exceeding its design capacity, a serviceability assessment becomes essential. This assessment often involves visual inspection, metrology, finite element analysis (FEA), and reviewing design documents [5]. While minor defects can sometimes be mitigated through temporary load reductions, these adjustments are short-term until scheduled maintenance allows for permanent rehabilitation [6]. Although replacing a CHS joint can restore structural integrity, it is rarely pursued due to logistical complexities, including accessibility and machinery requirements [7]. Traditional methods for strengthening tubular joints include welded steel collars, internal sleeves, and grouted connections. These methods offer unique benefits but have certain limitations in terms of durability, adaptability, and fatigue performance. For instance, welded collars enhance joint rigidity but risk introducing stress concentrations. Similarly, internal sleeves and grouted connections, though structurally robust, can be difficult to install, especially in offshore or remote locations [8].

Composite reinforcement has gained prominence due to its enhanced fatigue resistance, weight reduction, and long-term durability. Studies have shown that fiber-reinforced polymer (FRP) composites significantly improve the fatigue life of CHS structures by distributing stress more uniformly, thereby extending service life under cyclic loading [9,10]. Composite materials can be tailored to meet diverse strength and stiffness requirements, enabling their application in intricate profiles even in areas with limited accessibility, without the need for extensive inventories of repair materials [11]. Additionally, composite reinforcement offers advantages over welded stiffeners, including enhanced safety, on-site applicability without hot work, and suitability in high-temperature or underwater environments [12]. Its versatility in adapting to complex shapes and ease of on-site application make it an ideal choice for critical infrastructure, including offshore platforms and bridges.

The stress concentration factor (SCF) is a critical parameter used for fatigue life assessment via the structural hot-spot stress (HSS) approach, and various studies confirm composite reinforcement's efficacy in extending the fatigue life of CHS joints through SCF reduction [2]. These studies are listed in Table 1. However, most of the existing SCF models for composite-reinforced joints often fall short in predicting SCFs under multiplanar loads, which are common in real-world conditions, and are generally limited to specific joint

types [13]. Among these joint types, KT-joints are one of the most frequently used in offshore and civil structures due to their ability to accommodate multiple braces converging at different angles. Despite their importance, KT-joints remain relatively underexplored compared to simpler joint configurations such as T-, Y-, and X-joints. The multiplanar load paths and complex brace interactions in KT-joints result in highly non-uniform stress distributions, which existing SCF models fail to predict accurately. This gap necessitates further investigation to develop reliable SCF models specifically tailored to KT-joints, ensuring accurate fatigue life assessment and structural rehabilitation strategies. This research addresses these gaps by investigating SCF behavior under various loading scenarios in composite-reinforced KT-joints.

Table 1. Composite reinforcement of CHS joints.

Reference	Joint Type	Nature of Investigation
Hosseini et al. [14]	T/Y	Numerical and experimental
Tong et al. [15]	K	Experimental
Xu et al. [16]	K	Numerical and experimental
Hosseini et al. [17]	T/Y	Numerical and experimental
Nassirian et al. [18]	T/Y	Numerical
Hosseini et al. [19]	T/Y	Numerical
Hosseini et al. [20]	KT	Numerical
Nassiraei et al. [21]	X	Numerical
Xu et al. [22]	TT	Numerical and experimental
Mohamed et al. [23]	K	Numerical
Mohamed et al. [24]	T/Y	Numerical
Zavvar et al. [25]	DKT	Numerical
Zavvar et al. [26]	DKT	Numerical
Iqbal et al. [27]	KT	Numerical

2. Methodology

This research is based on numerical simulations using FEA. A parametric model of the KT-joint was simulated for various sizes covering a defined range. The simulation results were used to train an ANN and develop empirical equations. The KT-joint geometry was defined as a function of dimensionless parameters to simulate a wide range of designs and develop generalized empirical expressions. These parameters were based on those used in the literature to represent a wide range of design configurations [25]. These parameters are provided in Equations (1)–(7).

$$\beta = d/D \quad (1)$$

$$\gamma = D/2T \quad (2)$$

$$\tau = t/T \quad (3)$$

$$\alpha = 2L/D \quad (4)$$

$$\zeta = g/D \quad (5)$$

$$\eta = E_{frp}/E_{steel} \quad (6)$$

$$\epsilon = t_{FRP}/T_{chord} \quad (7)$$

where

D = chord diameter

d = brace diameter

T = thickness of chord wall

t = thickness of brace wall

L = length of chord

g = gap between braces at chord surface

E_{steel} = elastic modulus of steel (base joint)

E_{frp} = elastic modulus of reinforcement

t_{FRP} = thickness of reinforcement

A typical uniplanar KT-joint comprises one chord and three braces, as shown in Figure 2. Loads are usually transferred from the brace elements to the chord, and the chord transfers these loads to piles and foundations. Based on the practical considerations, the typical range of various parameters has been identified [28–33]. A set of possible design configurations was generated based on the geometric and reinforcement parameters $D, d, T, t, \theta, g, E_{frp}$, and t_{frp} . Analytical methods cannot be used to determine stress in complex geometries due to the complex stress behavior in tubular joints. Numerical methods, particularly FEM, are frequently used to determine the structural response of CHS joints [34]. Among various CAE software options, ANSYS Workbench 2024 R1 offers a user-friendly environment with advanced FE modeling and design exploration tools [35]. Various studies on CHS joints have successfully used ANSYS for the analysis of tubular joints [36]. The geometry of the KT-joint was modeled using ANSYS's DesignModeler. The geometry of the KT-joint was meshed with high-order solid elements using the ANSYS Structural mesh tool, and mesh convergence was ensured.

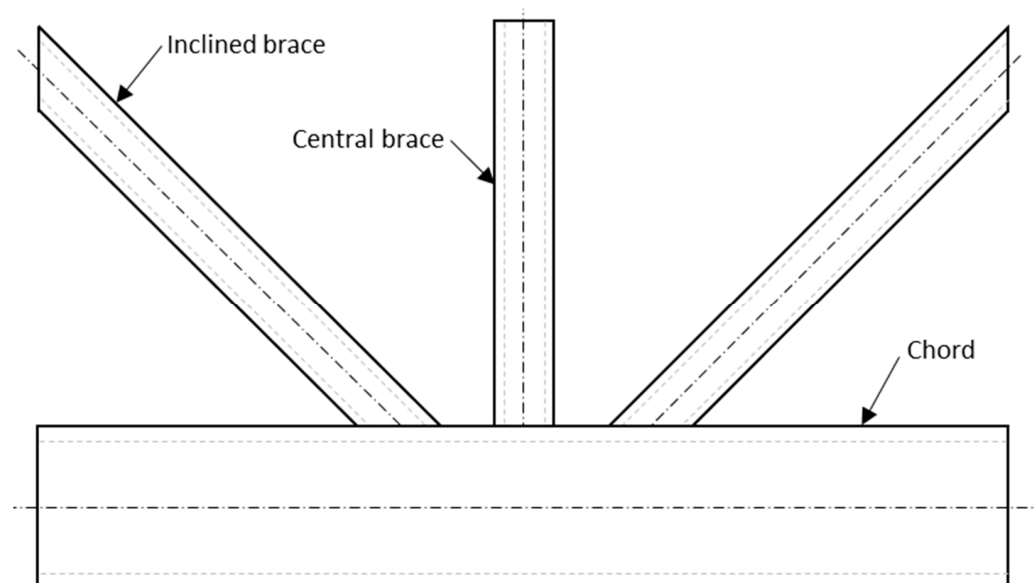


Figure 2. A typical KT-joint.

Steel with a modulus of elasticity and Poisson's ratio of 211 GPa and 0.3, respectively, was defined for all simulations [37]. Nonlinear material effects were not considered, as they do not influence SCF calculations. The hot-spot stress approaches operate within the elastic range. Both ends of the chord and inclined braces were fixed, and an axial compressive load was applied to the central brace of the KT-joint. Linear elastic analysis was carried out [38]. An artificial neural network (ANN) was configured with dimensionless parameters defining the joint geometry and reinforcement as the inputs, SCF along the weld toe as the output, and a hidden layer with multiple neurons. This model was trained using simulation results for the rapid estimation of SCF. Seventy percent of the simulation data set was used for training, fifteen percent for testing, and fifteen percent for validation.

3. Results and Discussion

A total of 5429 simulations were carried out for various design and reinforcement configurations. The coefficient of performance achieved for the best epoch was 0.9988, and the MSE was 0.0022. The trained function was exported and can be requested from the corresponding author. A KT-joint was tested experimentally to validate the trained function. A customized test rig was fabricated, as detailed in Iqbal et al. [39]. Static loads were applied to the central brace of the joint through a hydraulic jack, and the stress field was recorded using strain gauges installed on the chord surface at the interface. The maximum difference was less than 10 percent, as shown in Figure 3. According to the UK Department of Energy, empirical formulas with SCF prediction errors below 25% are considered acceptable [40]. If the deviation ranges between 25% and 50%, then a multiplication factor is recommended for correction. For errors exceeding 50%, a revision of the formula is required. Since the ANN predictions in this study show a maximum deviation of less than 10% compared to experimental results, the accuracy is well within the acceptable range.

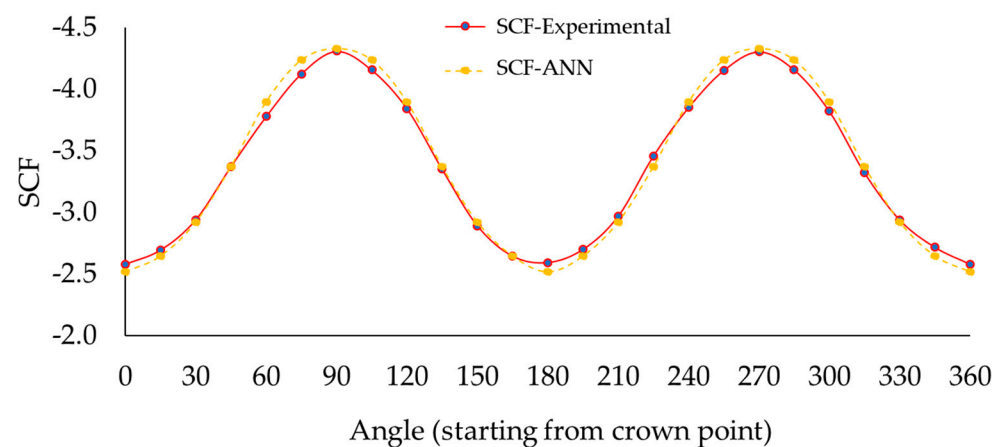


Figure 3. Comparison of experimental and ANN-based SCFs.

Furthermore, the variability of SCFs across different regions of the KT-joint was examined. The predictions showed consistent accuracy across critical joint locations, including the weld toe and saddle point regions, where SCFs are typically highest under axial compression. In both the unreinforced and composite-reinforced KT-joints, the accuracy remained within 10%, even at these high-SCF locations. While the magnitude of SCFs was reduced at various points in the composite-reinforced joint, the prediction accuracy remained within the acceptable deviation range for all locations.

While this study provides valuable insights into the prediction of SCFs in KT-joints, several areas remain for future investigation. One potential improvement is the inclusion of cyclic loading in the SCF predictions, which would better represent real-world conditions where structures are subjected to fluctuating loads over time. Additionally, the model can be further validated under multi-axial stress states, which are common in complex structural systems and could improve the accuracy of predictions in more varied loading scenarios. These aspects, along with potential refinements to the current model, will be explored in future work to enhance its applicability to a wider range of structural conditions.

4. Conclusions

This study demonstrated that stress concentration factors (SCFs) in circular hollow section (CHS) KT-joints can be significantly reduced using composite reinforcement, thereby enhancing the fatigue life of these structures. Furthermore, it was concluded that finite element analysis (FEA) combined with artificial neural networks (ANNs) provides a robust

approach to developing empirical models to approximate complex phenomena, such as SCF distribution along the weld toe. This enables accurate SCF estimation at critical locations, including the crown and saddle, facilitating precise hot-spot stress predictions in joints under combined loads. The trained ANN model exhibited excellent accuracy, with SCF estimations deviating by less than 10% from the simulation results.

Author Contributions: Conceptualization, S.K. and M.I. (Mohsin Iqbal); analysis, M.I. (Mohsin Iqbal) and A.R.; writing—original draft preparation, M.I. (Mohsin Iqbal); writing—review and editing, S.K., M.I. (Muhammad Iqbal), V.P. and M.O.; supervision, S.K. and V.P.; project administration, S.K.; funding acquisition, S.K. All authors have read and agreed to the published version of the manuscript.

Funding: This research received funding from Yayasan Universiti Teknologi PETRONAS under grant No. 015LC0-443.

Institutional Review Board Statement: Not applicable.

Informed Consent Statement: Not applicable.

Data Availability Statement: No new data were created or analyzed in this study. Data sharing is not applicable to this article.

Conflicts of Interest: The authors declare no conflict of interest.

References

1. Rabi, M.; Ferreira, F.P.V.; Abarkan, I.; Limbachiya, V.; Shamass, R. Prediction of the cross-sectional capacity of cold-formed CHS using numerical modelling and machine learning. *Results Eng.* **2023**, *17*, 100902. [\[CrossRef\]](#)
2. Iqbal, M.; Karuppanan, S.; Perumal, V.; Ovinis, M.; Iqbal, M.; Rasul, A. Optimization of fibre orientation for composite reinforcement of circular hollow section KT-joints. *Int. J. Struct. Integr.* **2024**, *15*, 717–730. [\[CrossRef\]](#)
3. Nichols, N.W.; Khan, R. Structural integrity management system (SIMS) implementation within PETRONAS' operations. *J. Mar. Eng. Technol.* **2015**, *14*, 61–69. [\[CrossRef\]](#)
4. Vieira Ávila, B.; Correia, J.; Carvalho, H.; Fantuzzi, N.; De Jesus, A.; Berto, F. Numerical analysis and discussion on the hot-spot stress concept applied to welded tubular KT joints. *Eng. Fail. Anal.* **2022**, *135*, 106092. [\[CrossRef\]](#)
5. Vinet, L.; Zhedanov, A. A “missing” family of classical orthogonal polynomials. *J. Phys. A Math. Theor.* **2011**, *44*, 085201. [\[CrossRef\]](#)
6. Dier, A.F. Background to new design manual for platform strengthening, modification and repair. In Proceedings of the Offshore Technology Conference, Houston, TX, USA, 6–9 May 1996; Volume 2, pp. 457–466. [\[CrossRef\]](#)
7. Deng, P.; Guo, J.; Zhu, Z.; Liu, Y.; Zhu, Q. Finite Element Analysis of Corrosion Tubular T-Joint Repaired with Grouted Clamp. *Adv. Civ. Eng.* **2023**, *2023*, 6634023. [\[CrossRef\]](#)
8. Souza, M.; Bayazitoglu, Y.; Lu, L.S.; Valdes, V.; Vazquez, R. Repairs of hurricane damaged platforms in the Bay of Campeche. In Proceedings of the Offshore Technology Conference, Houston, TX, USA, 4–7 May 1997; Volume 3, pp. 107–116. [\[CrossRef\]](#)
9. ASME PCC-2; Repair of Pressure Equipment and Piping. ASME: New York, NY, USA, 2011.
10. ISO 24817; Petroleum, Petrochemical and Natural Gas Industries—Composite Repairs for Pipework—Qualification and Design, Installation, Testing and Inspection. International Standard Organization: Geneva, Switzerland, 2015.
11. Perrut, V.A.; Meniconi, L.C.d.M.; Sampaio, E.M.; Rohem, N.R.F.; da Costa, M.F. Fatigue and quasi-static analysis of a new type of surface preparation used for the CFRP repair of steel offshore structures. *J. Adhes.* **2019**, *95*, 849–873. [\[CrossRef\]](#)
12. De Barros, S.; Banea, M.D.; Budhe, S.; De Siqueira, C.E.R.; Lobão, B.S.P.; Souza, L.F.G. Experimental analysis of metal-composite repair of floating offshore units (FPSO). *J. Adhes.* **2017**, *93*, 147–158. [\[CrossRef\]](#)
13. Iqbal, M.; Karuppanan, S.; Perumal, V.; Ovinis, M.; Nouman, H. Empirical modeling of stress concentration factors using finite element analysis and artificial neural networks for the fatigue design of tubular KT-joints under combined loading. *Fatigue Fract. Eng. Mater. Struct.* **2023**, *46*, 4333–4349. [\[CrossRef\]](#)
14. Sadat Hosseini, A.; Bahaari, M.R.; Lesani, M. Stress concentration factors in FRP-strengthened offshore steel tubular T-joints under various brace loadings. *Structures* **2019**, *20*, 779–793. [\[CrossRef\]](#)
15. Tong, L.; Xu, G.; Zhao, X.L.; Zhou, H.; Xu, F. Experimental and theoretical studies on reducing hot spot stress on CHS gap K-joints with CFRP strengthening. *Eng. Struct.* **2019**, *201*, 296–313. [\[CrossRef\]](#)
16. Xu, G.; Tong, L.; Zhao, X.L.; Zhou, H.; Xu, F. Numerical analysis and formulae for SCF reduction coefficients of CFRP-strengthened CHS gap K-joints. *Eng. Struct.* **2020**, *210*, 369–386. [\[CrossRef\]](#)
17. Sadat Hosseini, A.; Bahaari, M.R.; Lesani, M. Experimental and parametric studies of SCFs in FRP strengthened tubular T-joints under axially loaded brace. *Eng. Struct.* **2020**, *213*, 110548. [\[CrossRef\]](#)

18. Nassiraei, H.; Rezadoost, P. Stress concentration factors in tubular T/Y-joints strengthened with FRP subjected to compressive load in offshore structures. *Int. J. Fatigue* **2020**, *140*, 105719. [\[CrossRef\]](#)
19. Hosseini, A.S.; Bahaari, M.R.; Lesani, M. SCF distribution in FRP-strengthened tubular T-joints under brace axial loading. *Sci. Iran.* **2020**, *27*, 1113–1129. [\[CrossRef\]](#)
20. Sadat Hosseini, A.; Zavvar, E.; Ahmadi, H. Stress concentration factors in FRP-strengthened steel tubular KT-joints. *Appl. Ocean Res.* **2021**, *108*, 1187–1221. [\[CrossRef\]](#)
21. Nassiraei, H.; Rezadoost, P. Development of a probability distribution model for the SCFs in tubular X-connections retrofitted with FRP. *Structures* **2022**, *36*, 233–247. [\[CrossRef\]](#)
22. Xu, X.; Shao, Y.; Gao, X.; Mohamed, H.S. Stress concentration factor (SCF) of CHS gap TT-joints reinforced with CFRP. *Ocean Eng.* **2022**, *247*, 110722. [\[CrossRef\]](#)
23. Mohamed, H.S.; Zhang, L.; Shao, Y.B.; Yang, X.S.; Shaheen, M.A.; Suleiman, M.F. Stress concentration factors of CFRP-reinforced tubular K-joints via Zero Point Structural Stress Approach. *Mar. Struct.* **2022**, *84*, 103239. [\[CrossRef\]](#)
24. Mohamed, H.S.; Yang, X.S.; Shao, Y.B.; Shaheen, M.A.; Suleiman, M.F.; Zhang, L.; Hossian, A. Stress concentration factors (SCF) of CFRP-reinforced T/Y-joints via ZPSS approach. *Ocean Eng.* **2022**, *261*, 112092. [\[CrossRef\]](#)
25. Zavvar, E.; Henneberg, J.; Guedes Soares, C. Stress concentration factors in FRP-reinforced tubular DKT joints under axial loads. *Mar. Struct.* **2023**, *90*, 429–452. [\[CrossRef\]](#)
26. Zavvar, E.; Sousa, F.; Giannini, G.; Taveira-Pinto, F.; Santos, P.R. Probability of maximum values of stress concentration factors in tubular DKT-joints reinforced with FRP under axial loads. *Structures* **2024**, *66*, 106809. [\[CrossRef\]](#)
27. Iqbal, M.; Karuppanan, S.; Perumal, V.; Ovinis, M.; Khan, A. Stress Concentration Factors in CFRP-Reinforced KT-Joints under Multiplanar Bending Loads: Experimental and Numerical Investigation. *Results Eng.* **2025**, *25*, 103745. [\[CrossRef\]](#)
28. Smedley, P.; Fisher, P. *Stress Concentration Factors for Simple Tubular Joints*; Offshore Technology Report; Health and Safety Executive: London, UK, 1991.
29. ARSEM. *Design Guides for Offshore Structures—Welded Tubular Joints*; Technip: Paris, France, 1987; Volume 1.
30. American Petroleum Institute (API). *Recommended Practice for Planning D and CFOP-WSD. API RP 2A WSD*, 22nd ed.; API Publishing Services: Washington, DC, USA, 2014; Volume 2014.
31. Ahmadi, H.; Ziyaei Nejad, A. Stress Concentration Factors in Uniplanar Tubular KT-Joints of Jacket Structures Subjected to In-Plane Bending Loads. *Int. J. Marit. Technol.* **2016**, *5*, 27–39.
32. Ahmadi, H. Probabilistic analysis of the DoB in axially-loaded tubular KT-joints of offshore structures. *Appl. Ocean Res.* **2019**, *87*, 64–80. [\[CrossRef\]](#)
33. Moffat, D.G.; Kruselecki, J.; Blachut, J. The Effects of Chord Length and Boundary Conditions on the Static Strength of a Tubular T-Joint under Brace Compression Loading. *Mar. Struct.* **1996**, *9*, 935–947. [\[CrossRef\]](#)
34. Zhao, X.-L.; Packer, J.A. *Fatigue Design Procedure for Welded Hollow Section Joints*, 1st ed.; Abington Publishing: Cambridge, UK, 2000. [\[CrossRef\]](#)
35. Chen, X.; Liu, Y. *Finite Element Modeling and Simulation with ANSYS Workbench*; CRC Press: Boca Raton, FL, USA, 2015. [\[CrossRef\]](#)
36. Zavvar, E.; Rosa-Santos, P.; Ghafoori, E.; Taveira-Pinto, F. Analysis of tubular joints in marine structures: A comprehensive review. *Mar. Struct.* **2025**, *99*, 103702. [\[CrossRef\]](#)
37. Zhang, Y.; Zhang, K.; Zhao, H.; Xin, J.; Duan, M. Stress analysis of adhesive in a cracked steel plate repaired with CFRP. *J. Constr. Steel Res.* **2018**, *145*, 210–217. [\[CrossRef\]](#)
38. N'Diaye, A.; Hariri, S.; Pluvinaige, G.; Azari, Z. Stress concentration factor analysis for notched welded tubular T-joints. *Int. J. Fatigue* **2007**, *29*, 1554–1570. [\[CrossRef\]](#)
39. Iqbal, M.; Karuppanan, S.; Perumal, V.; Ovinis, M.; Iqbal, M. Design and Testing of a Test Rig for Tubular Joints Hot-Spot Stress Determination. *Results Eng.* **2025**, *25*, 103931. [\[CrossRef\]](#)
40. Health & Safety Executive (HSE). *Background to New Fatigue Guidance for Steel Joints and Connections in Offshore Structures*; Health & Safety Executive: Sudbury, UK, 1999; pp. 1–123.

Disclaimer/Publisher’s Note: The statements, opinions and data contained in all publications are solely those of the individual author(s) and contributor(s) and not of MDPI and/or the editor(s). MDPI and/or the editor(s) disclaim responsibility for any injury to people or property resulting from any ideas, methods, instructions or products referred to in the content.